The reaction $\pi N \to \pi\pi N$ above threshold in heavy-baryon chiral perturbation theory

J. Zhang and N. Mobed*
Department of Physics
University of Regina
Regina, SK S4S 0A2, Canada

M. Benmerrouche
Saskatchewan Accelerator Laboratory
University of Saskatchewan
Saskatoon, SK S7N 5C6, Canada

We study the reactions $\pi^{\pm}p \to \pi^{\pm}\pi^{+}n$ and $\pi^{-}p \to \pi^{o}\pi^{o}n$ in heavy-baryon chiral perturbation theory of chiral order three from threshold up to pion laboratory kinetic energies of 400 MeV. We find that the contributions from amplitudes of chiral order three are large and play an essential role in reproducing the experimental data.

PACS numbers: 25.80.Hp, 12.39.Fe, 11.30.Rd
Keywords: Chiral Perturbation Theory, π-N interactions

*Corresponding Author
E-mail: mobed@meena.cc.uregina.ca
Fax: (306)-585-4894
Tel: (306)-585-4359

The reaction $N(\pi, 2\pi)N$ has been the subject of a number of experimental [1,2] and theoretical [3–8] investigations. The reaction is of interest in connection with various aspects of chiral symmetry and its spontaneous breaking, including a determination of π-π scattering amplitude and the study of non-linear realization of chiral symmetry. The theoretical work on the reaction $N(\pi, 2\pi)N$ may be broadly divided into two categories. In one category, calculations are based on a tree-level chiral Lagrangian and include meson and baryon resonances as explicit degrees of freedom [3–5]. While these models capture the physical essence of the reaction under consideration, they are not consistent with the power-counting scheme of Chiral Perturbation Theory (ChPT) [9,10]. The second category includes calculations which are fully within the framework of the baryon ChPT. In [6] the lowest order ($O(q)$) relativistic Lagrangian was employed, while in [8] the calculations were performed in the next-to-leading order ($O(q^2)$) relativistic framework. The power counting ambiguities of the relativistic formalism are discussed in [9]. Heavy-Baryon Chiral Perturbation Theory (HBChPT) circumvents these difficulties [11,12]. The most comprehensive study of the reaction $N(\pi, 2\pi)N$ at the threshold was carried out in [7], where a complete $O(q^3)$ calculation was performed in HBChPT. The purpose of this paper is to investigate the reaction $N(\pi, 2\pi)N$ beyond the threshold in HBChPT up to $O(q^3)$. Technically, the threshold and beyond the threshold calculations differ in two respects. First, as one moves away from threshold the number of Feynman diagrams increases significantly. Second, the evaluation of loop integrals becomes more involved.

Our starting point is the low energy expansion of the πN chiral Lagrangian in HBChPT as described in detail in Ref. [13]. The effective chiral Lagrangian may be expanded as

$$\mathcal{L}_{\rm eff} = \mathcal{L}_\pi^{(2)} + \mathcal{L}_\pi^{(4)} + \cdots + \mathcal{L}_{\pi N}^{(1)} + \mathcal{L}_{\pi N}^{(2)} + \mathcal{L}_{\pi N}^{(3)} + \cdots , \tag{1}$$

where the superscripts denote the chiral order in the standard power counting scheme [11,12]. In order to obtain amplitudes of $O(q^3)$, the pion and the pion-nucleon Lagrangians may be truncated at $O(q^4)$ and $O(q^3)$, respectively. The pion $\mathcal{L}_\pi^{(i)}$, and the pion-nucleon, $\mathcal{L}_{\pi N}^{(i)}$ parts of the Lagrangian are discussed in detail in [9] and [13], respectively. In the absence of external fields and in the isospin symmetric limit, the pertinent pieces of the Lagrangian assume the following form:

$$\mathcal{L}_\pi^{(2)} = \frac{F^2}{4}\langle u\cdot u\rangle + \frac{1}{2}m_\pi^2 F^2 \langle U\rangle\,, \tag{2}$$

$$\begin{aligned}\mathcal{L}_\pi^{(4)} = \frac{1}{16}\Big\{&4l_1\langle u\cdot u\rangle^2 + 4l_2\langle u_\mu u^\nu\rangle\langle u^\mu u_\nu\rangle + l_3\langle\chi_+\rangle^2 \\ &+l_4(2\langle\chi_+\rangle\langle u\cdot u\rangle + 2\langle\chi_-^2\rangle - \langle\chi_-\rangle^2)\Big\}\,,\end{aligned} \tag{3}$$

$$\mathcal{L}_{\pi N}^{(1)} = \overline{N}_v \left(iv\cdot\nabla + g_A S\cdot u\right) N_v\,, \tag{4}$$

$$\begin{aligned}\mathcal{L}_{\pi N}^{(2)} = \overline{N}_v\,\Big\{&-\frac{1}{2M}\left(\nabla^2 + ig_A\{u\cdot v, S\cdot\nabla\}\right) + \frac{a_1}{M}\langle u\cdot u\rangle + \frac{a_2}{M}\langle (u\cdot v)^2\rangle \\ &+\frac{m_\pi^2 a_3}{M}\langle U+U^\dagger\,\rangle + \frac{m_\pi^2 a_4}{M}\left(U+U^\dagger - \frac{1}{2}\langle U+U^\dagger\,\rangle\right)\end{aligned}$$

$$+\frac{ia_5}{M}\epsilon^{\mu\nu\alpha\beta}v_\alpha S_\beta\, u_\mu u_\nu\Big\}\, N_v\,, \tag{5}$$

$$\begin{aligned}
\mathcal{L}^{(3)}_{\pi N} &= \frac{g_A}{8M^2}\,\overline{N}_v\,\Big[\nabla_\mu,\Big[\nabla^\mu, S\cdot u\Big]\Big]\; N_v \\
&+\frac{1}{2M^2}\overline{N}_v\,\Big\{-\left(a_5-\frac{1-3g_A^2}{8}\right)\,u_\mu u_\nu \epsilon^{\mu\nu\alpha\beta}S_\beta\nabla_\alpha+\frac{g_A}{2}S\cdot\nabla u\cdot\nabla \\
&\qquad -\frac{g_A^2}{8}\,\{v\cdot u, u_\mu\}\,\epsilon^{\mu\nu\alpha\beta}v_\alpha S_\beta\nabla_\nu+\text{h.c.}\Big\}\,N_v+\frac{1}{(4\pi F)^2}\overline{N}_v\left(\sum_{i=1}^{24}b_i O_i\right)N_v.
\end{aligned} \tag{6}$$

Here, $S^\mu=\frac{i}{2}\gamma_5\sigma^{\mu\nu}v_\nu$ is the spin matrix, $U=u^2=\exp(i\vec{\tau}\cdot\vec{\pi}/F)$ is the SU(2) pion field with F being the pion decay constant, and $N_v(x)$ is the velocity-dependent nucleon field defined in terms of the Dirac spinor, $\psi(x)$, as

$$N_v(x)=e^{iMv\cdot x}\frac{1}{2}(1+\not{v})\psi(x), \tag{7}$$

where M is the nucleon mass, and the four-velocity v^μ satisfies the constraint $v^2=1$. The last term in $\mathcal{L}^{(3)}_{\pi N}$ involving the Low Energy Constants (LECs) b_i is usually referred to as the counterterm Lagrangian. Some of the coefficients l_i and b_i are divergent in order to absorb the divergences of the one-loop diagrams which start contributing at order $O(q^3)$. In the dimensional regularization scheme, these low energy constants l_i and b_i can be decomposed as [14]:

$$l_i=l_i^r(\mu)+\gamma_i\Lambda,\quad b_i=b_i^r(\mu)+(4\pi)^2\beta_i\Lambda, \tag{8}$$

and

$$\Lambda=\frac{1}{32\pi^2}\left[\frac{2}{(d-4)}-\ln(4\pi)-\Gamma'(1)-1\right], \tag{9}$$

where $l_i^r(\mu)$ and $b_i^r(\mu)$ are the renormalized values of l_i and b_i at the scale μ. Ecker and Mojžiš [13] have worked out the counterterms and their β–functions involved in $\mathcal{L}^{(3)}_{\pi N}$ and we refer to their paper for the explicit form of the operators O_i and the coefficients β_i. The coefficients γ_i are given in [9,15] . We have also used the standard notation for the operators $\chi=(m_u+m_d)B_0=m_\pi^2$, $u_\mu=i(u^\dagger\partial_\mu u-u\partial_\mu u^\dagger)$, $\nabla=\partial+\Gamma$ and $\Gamma_\mu=\frac{1}{2}(u^\dagger\partial_\mu u+u\partial_\mu u^\dagger)$. By expanding the field $U=u^2$ in powers of the pion field and substituting the result in the effective Lagrangian, we obtain an explicit form of the Lagrangian suitable for deriving the Feynman rules. To a given chiral order, the transition amplitude $\mathcal{T}_{fi}$ receives contributions from all the possible connected Feynman diagrams up to that order. The (non-vanishing) topologically distinct diagrams of up to $O(q^3)$ contributing to the reaction $N(\pi,2\pi)N$ are given in Fig. 1. The self-energy diagrams are not shown. It is worth emphasizing that the actual number of diagrams for any particular physical channel is much greater than that of the ones displayed in Fig. 1. The individual Feynman graphs of $O(q^3)$ are not necessarily finite, but the total transition amplitude is finite at each order.

Before presenting our results we have to make a few remarks on the input parameters of our calculations. For the reaction under consideration up to $O(q^3)$ the following vertices and

LECs are needed: $\mathcal{L}_\pi^{(2)}$ involving m_π and F_π, $\mathcal{L}_\pi^{(4)}$ with LECs l_i $(i=1,\cdots,4)$, $\mathcal{L}_{\pi N}^{(1)}$ containing g_A, $\mathcal{L}_{\pi N}^{(2)}$ containing M and a_1 through a_5, and finally $\mathcal{L}_{\pi N}^{(3)}$, containing 24 LECs b_i of which 14 can, in principle, contribute to the reaction under consideration. Of the 14 LECs, 5 combinations containing 9 LECs contribute to the πN elastic scattering; these combinations have been recently determined [15]. The remaining LECs needed in our calculation are $b_4, b_{11}, b_{12}, b_{13}, b_{14}, b_{17}$. In this work, we treat the finite part of the unknown LECs as free parameters and denote them by $\tilde{b}_i$. The numerical values of a_i and $\tilde{b}_i$ are listed in Tables I and II, respectively. Throughout the calculations the physical values of the quantities m_π, F_π, g_A and M are used. As discussed in [15] this amounts to corrections of $O(q^3)$ and higher. The corrections of $O(q^3)$ are explicitly included in the amplitudes of the same order.

In HBChPT the transition amplitude for the reaction

$$\pi(q) + N(p = Mv + l_i) \longrightarrow \pi(q_1) + \pi(q_2) + N(p' = Mv + l_f) \tag{10}$$

can be written as

$$\mathcal{T}_{fi} = \bar{u}_v^{(\alpha_f)}(l_f)\, \mathcal{A}\, u_v^{(\alpha_i)}(l_i), \tag{11}$$

in which $u_v^{(\alpha)}(l)$ denotes the heavy baryon spinor with residual momentum l and spin projection α. We find that the amplitude $\mathcal{A}$ has the following Lorentz structure

$$\mathcal{A} = A_0\, S\cdot q + A_1\, S\cdot q_1 + A_2\, S\cdot q_2 + i\epsilon_{\alpha\beta\mu\nu} v^\alpha q^\beta q_1^\mu q_2^\nu B, \tag{12}$$

where A_i $(i=0,1,2)$ and B are invariant functions of external momenta.

In order to make contact with the experimental data, we need to relate the frame-dependent HBChPT amplitudes to the relativistic invariant amplitudes. The relativistic amplitude for the reaction $N(\pi, 2\pi)N$ can be parameterized as [5,6]:

$$\mathcal{M}_{fi} = \overline{u}(p')\, \gamma_5 \left[f_1 + f_2\, \not{q}_1 + f_3\, \not{q}_2 + f_4\, \not{q}_1\, \not{q}_2 \right] u(p). \tag{13}$$

The use of (12) and (13), along with the matching condition introduced in [16] results in the following relations between the relativistic and heavy-baryon amplitudes:

$$\begin{aligned} f_1 = {} & M\left(1 - \frac{t}{4M^2}\right)(A_0 - 2B\, q_1\cdot q_2) + \frac{1}{2}(A_0 + A_1)\, v\cdot q_1 + \frac{1}{2}(A_0 + A_2)\, v\cdot q_2 \\ & + \left[v\cdot q_1\, q\cdot q_2 - v\cdot q_2\, q\cdot q_1 + v\cdot(q_2 - q_1)\,(m_\pi^2 + q_1\cdot q_2)\right] B, \end{aligned} \tag{14}$$

$$f_2 = -\frac{1}{2}(A_0 + A_1)\; - \left[2M\, v\cdot q_2 + q_2\cdot(q - q_1) - m_\pi^2 \right] B, \tag{15}$$

$$f_3 = -\frac{1}{2}(A_0 + A_2)\; + \left[2M\, v\cdot q_1 + q_1\cdot(q - q_2) - m_\pi^2 \right] B, \tag{16}$$

$$f_4 = 2M\left(1 - \frac{t}{4M^2}\right) B, \tag{17}$$

where $t = (p - p')^2$. At threshold the relativistic transition amplitude takes a simple form:

$$\mathcal{M}_{fi} = a\, \chi^{(\alpha_f)^\dagger}\, \vec{\sigma}\cdot\vec{q}\, \chi^{(\alpha_i)}, \tag{18}$$

where

$$a = \frac{1}{2M}\left[m_\pi\,(f_2+f_3) - f_1 - m_\pi^2\,f_4\right]. \tag{19}$$

The threshold amplitudes corresponding to a well-defined isospin channel, commonly referred to as $a^{3,2}$ and $a^{1,0}$, can be decomposed in terms of physical amplitudes [5]:

$$a^{1,0} = \frac{3}{\sqrt{2}}\,a^{\pi^0\pi^0 n} - \frac{1}{\sqrt{2}}\,a^{\pi^+\pi^+ n}, \tag{20}$$

$$a^{3,2} = \frac{\sqrt{5}}{2}\,a^{\pi^+\pi^+ n}, \tag{21}$$

where $a^{\pi^0\pi^0 n}$ and $a^{\pi^+\pi^+ n}$ are the threshold amplitudes for the physical reactions $\pi^- p \to \pi^0\pi^0 n$ and $\pi^+ p \to \pi^+\pi^+ n$ respectively. Furthermore, the amplitudes D_1, D_2 defined by Bernard, Kaiser, Meißner (BKM) [7] are related to $a^{i,j}$ by

$$D_1 = \frac{1}{\sqrt{10}}\,a^{3,2}, \tag{22}$$

$$D_2 = -\frac{2}{3}\,\frac{a^{3,2}}{\sqrt{10}} - \frac{1}{3}\,a^{1,0}. \tag{23}$$

Our numerical results for D_1 and D_2 up to chiral order $O(q^3)$ are listed in Tables III and IV. Clearly the contribution of non-leading terms to the threshold amplitudes are substantial, and the results seem to be sensitive to the values of the unknown LECs. Our calculated values of D_1 and D_2 seem to be in fair agreement with the data. These statements are somewhat tentative in that the use of the actual values of the unknown LECs may lead to a different set of conclusions. The HBChPT calculations of BKM, on the other hand, are in impressive agreement with the data. In principle, the difference between our predictions and those of BKM is a consequence of using different values of LECs $\tilde{b}_i$. In their work, BKM estimated the contribution of the terms containing the unknown LECs using the resonance saturation method [7]. As such, there are no free parameters in their calculations. It is conceivable that with a systematic variation of the unknown LECs we may also obtain a good agreement with the data. Finally, we note that the calculations of Ref. [5], while not fully consistent with the principles of chiral perturbation theory, yield results which are in close agreement with our calculations.

We now turn our attention to the total cross sections. The spin-averaged cross-section is given by

$$\sigma = \frac{2M}{4s\,[(p\cdot q)^2 - M^2 m_\pi^2]^{1/2}} \int \overline{|\mathcal{T}_{fi}|^2}\,\frac{d^3p'}{(2\pi)^3}\,\frac{M}{E_{p'}}\,\frac{d^3q_1}{(2\pi)^3 2\omega_{q_1}}\,\frac{d^3q_2}{(2\pi)^3 2\omega_{q_2}}(2\pi)^4\delta^4(P_f - P_i), \tag{24}$$

where s is a statistical factor accounting for the existence of identical particles in the final state. Using (12), we obtain

$$\overline{|\mathcal{T}_{fi}|^2} = C(p)C(p')\left\{\frac{1}{4}(v\cdot A\, v\cdot A^* - |A|^2) + \left(\epsilon_{\alpha\beta\mu\nu}v^\alpha q^\beta q_1^\mu q_2^\nu\right)^2 |B|^2\right\}, \tag{25}$$

where $C(p) \equiv \dfrac{v\cdot p + M}{2M}$. To compute the cross-section, one has to integrate (25) over an appropriate phase-space. The phase-space integration was carried out numerically using a Monte-Carlo routine GENBOD from the CERN program library [17]. It is worth noting that while the transition amplitude is evaluated in the isospin limit, physical masses are used for the reaction kinematics.

The calculations have been performed for the Lab incident pion kinetic energy, T_π, from threshold up to 400 MeV. From a theoretical point of view, chiral perturbation theory is expected to be more reliable at low energies. Hence, for each reaction, we shall present our results for two kinematic domains: from threshold to 200 MeV, and from threshold to 400 MeV. Furthermore, to facilitate comparison among different chiral orders, results will be displayed order by order in the chiral expansion. Finally, in order to study the sensitivity of the results to the values of the unknown LECs, $\tilde{b}_i$, we have performed three sets of calculation for each reaction: all unknown $\tilde{b}_i = 0$, unknown $\tilde{b}_i = 10$, and unknown $\tilde{b}_i = -10$. The choice of the range of variation of the unknown $\tilde{b}_i$ is based on the reported values of the known LECs $\tilde{b}_i$ as listed in Table II. Some of the known LECs in Table II have rather large uncertainties. It was found that the cross-sections are not noticeably affected by these uncertainties. Our results are illustrated in Figs. 2 and 3.

Our main results can be summarized as follows. The leading order amplitudes consistently underestimate the experimental results by a large amount over most of the kinematic range considered in our calculations. The inclusion of terms of $O(q^2)$ produces only a small change in the cross-section. The contribution of terms of $O(q^3)$, on the other hand, is quite large and in general results in an improved agreement with the data. From a phenomenological point of view these observations can be regarded as a success for HBChPT. However, from a theoretical point of view, the fact that the contribution of terms of order $O(q^3)$ is much larger than that of the lower order terms, is indicative of the slow rate of convergence of HBChPT. The slow convergence of HBChPT has also been observed [11,15] for processes other than $N(\pi, 2\pi)N$. The lack of knowledge about the values of a number of LECs, $\tilde{b}_i$, is the main source of uncertainty in our calculations. Our results suggest that variations in $\tilde{b}_i$ can produce quite noticeable effects in observables considered here. Clearly a systematic investigation is necessary in order to determine or constrain the unknown LECs. So far as the reaction $N(\pi, 2\pi)N$ is concerned, one could try to fit the total cross-section in conjunction with a number of more sensitive differential cross-section and angular correlation data. These investigations are beyond the scope of the present work and will be the subject of a future publication.

To conclude, we note that our quantitative results for the total cross-section are in fair agreement with previous calculations for the reaction $N(\pi, 2\pi)N$) [3–6,8]. The fundamental difference between the present work and the previous ones is the calculational framework employed. Our calculations are performed in HBChPT and hence obey a consistent chiral power counting scheme.

This work has been supported by the Natural Sciences and Engineering Research Council of Canada.

[1] M.D. Manley, Phys. Rev. D 30 (1984) 536 and references cited therein.
[2] D. Počanić et al., Phys. Rev. Lett. 72 (1993) 1156 and references cited therein.
[3] E. Oset and M.J. Vicente–Vacas, Nucl. Phys. A 446 (1985) 584.
[4] O. Jäkel, H.W. Ortner, M. Dillig and C.A.Z. Vasconcellos, Nucl. Phys. A 511 (1990) 733; and C.A.Z. Vasconcellos, Nucl. Phys. A 541 (1992) 675; O. Jäkel and M. Dillig, Nucl. Phys. A 561 (1993) 557.
[5] T.S. Jensen and A. Miranda, πN Newsletter 10 (1995) 10; T.S. Jensen and A. Miranda, Phys. Rev. C 55 (1997) 1039.
[6] J. Beringer, πN Newsletter 7 (1992) 33.
[7] V. Bernard, N. Kaiser and Ulf-G. Meißner, Nucl. Phys. B 457 (1995) 147.
[8] V. Bernard, N. Kaiser and Ulf-G. Meißner, Nucl. Phys. A 619 (1997) 261.
[9] J. Gasser, M.E. Sainio and A. Švarc, Nucl. Phys. B 307 (1998) 779.
[10] A. Krause, Helv. Acta Phys. 63 (1990) 3.
[11] V. Bernard, N. Kaiser and Ulf-G. Meißner, Int. J. Mod. Phys. E 4 (1995) 193.
[12] G. Ecker, Prog. Part. Nucl. Phys. 35 (1995) 1.
[13] G. Ecker and M. Mojžiš, Phys. Lett. B 365 (1996) 312.
[14] J.F. Donoghue, E. Golowich and B.R. Holstein, Dynamics of the Standard Model, (Cambridge University Press 1992).
[15] M. Mojžiš, Eur. Phys. J. C2 (1998) 181.
[16] G. Ecker and M. Mojžiš, Phys. Lett. B 410 (1997) 266.
[17] F. James, GENBOD: N-Body Monte-Carlo Event Generator, CERN Computer Centre Program Library (1975).
[18] H. Burkhardt and J. Lowe, Phys. Rev. Lett 72 (1991) 2622; πN Newsletter 8 (1993) 173.
[19] M. Sevior et al., Phys. Rev. Lett. 66 (1991) 2569.
[20] G. Kernel et al., Z. Phys. C 48 (1990) 201.
[21] J. Kirz, J. Schwartz and R.D. Tripp, Phys. Rev. 126 (1962) 763.
[22] G. Kernel et al., Phys. Lett. B 216 (1989) 244; ibid B 225 (1989) 198.
[23] C.W. Bjork et al., Phys. Rev. Lett. 44 (1980) 62.
[24] M. Sevior et al., πN Newsletter 13 (1997) 32.
[25] J. Lowe et al., Phys. Rev. C44 (1991) 956.

Fig. 1: Topologically distinct graphs contributing to the $\pi N \to \pi\pi N$ reaction up to chiral order $O(q^3)$. Self-energy diagrams and diagrams which give zero contribution are not shown.

Fig. 2: The total cross section in the threshold region for $\pi^+ p \to \pi^+\pi^+ n$, $\pi^- p \to \pi^+\pi^- n$ and $\pi^- p \to \pi^o\pi^o n$ reactions. The long dashed curve is our prediction to chiral order $O(q)$, the dashed-dotted curve corresponds to $O(q) + O(q^2)$, the solid curve is the complete calculation $O(q) + O(q^2) + O(q^3)$ with all unknown LECs set to zero. The dotted and short dashed curves show the sensitivities to upward and downward shifts of all the unknown LECs by 10 units, respectively. The experimental data are represented by the symbols: Filled diamonds: [19], empty triangles: [20], Filled squares: [21], Filled circles: [22], Empty circles: [23], Stars: [24], Filled Triangles: [25].

Fig. 3: Same as Fig. 2 but for a wider kinematic range.

TABLE I. The LECs contributing to amplitudes of $O(q^2)$ or higher [15]

a_1	a_2	a_3	a_5
-2.60 ± 0.03	1.40 ± 0.05	-1.00 ± 0.06	3.30 ± 0.05

TABLE II. The LECs contributing to amplitudes of $O(q^3)$ [9,15]

$\bar{l}_1$	$\bar{l}_2$	$\bar{l}_3$	$\bar{l}_4$
-2.3 ± 3.7	6.0 ± 1.3	2.9 ± 2.4	4.3 ± 0.9

$\tilde{b}_1 + \tilde{b}_2$	$\tilde{b}_3$	$\tilde{b}_6$	$\tilde{b}_{15} - \tilde{b}_{16}$	$\tilde{b}_{19}$
2.4 ± 0.3	-2.8 ± 0.6	1.4 ± 0.3	-6.1 ± 0.4	-2.4 ± 0.2

TABLE III. Calculated values of D_1 and D_2 in this work

	$O(q)$	$O(q^2)$	$O(q^3)$, ($\tilde{b}_i = 0$)	$O(q^3)$, ($\tilde{b}_i = 10$)	$O(q^3)$, ($\tilde{b}_i = -10$)
$D_1(\mathrm{fm}^3)$	2.50	2.14	2.04	0.50	4.46
$D_2(\mathrm{fm}^3)$	-7.70	-6.96	-10.88	-8.92	-13.95

TABLE IV. Values of D_1 and D_2

	Experiment [18]	Present Work $O(q^3)$, ($\tilde{b}_i = 0$)	Theory [7]	Theory [5]
$D_1(\mathrm{fm}^3)$	2.26 ± 0.12	2.04	2.65 ± 0.24	1.87
$D_2(\mathrm{fm}^3)$	-9.05 ± 0.36	-10.88	-9.06 ± 1.05	-10.58

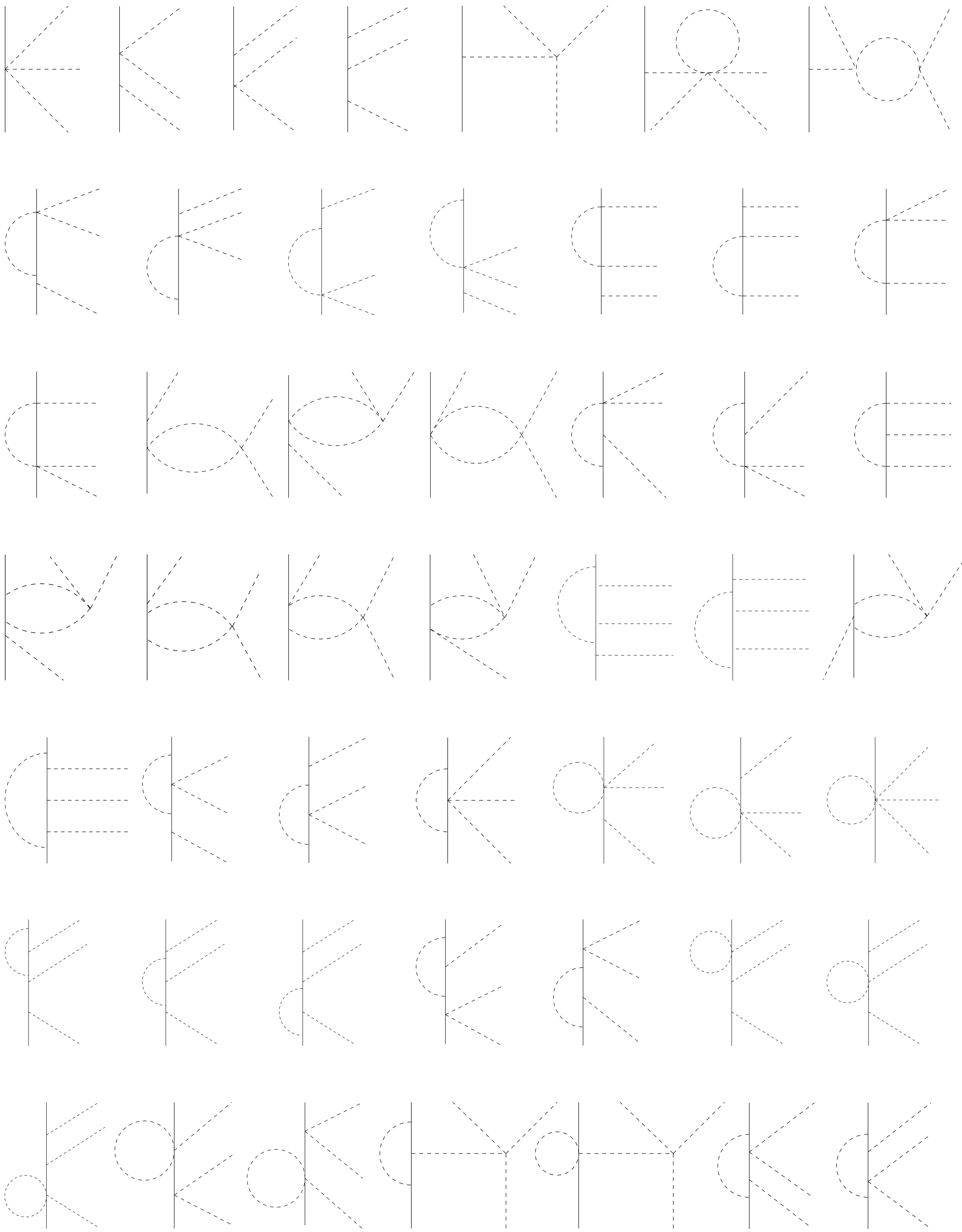

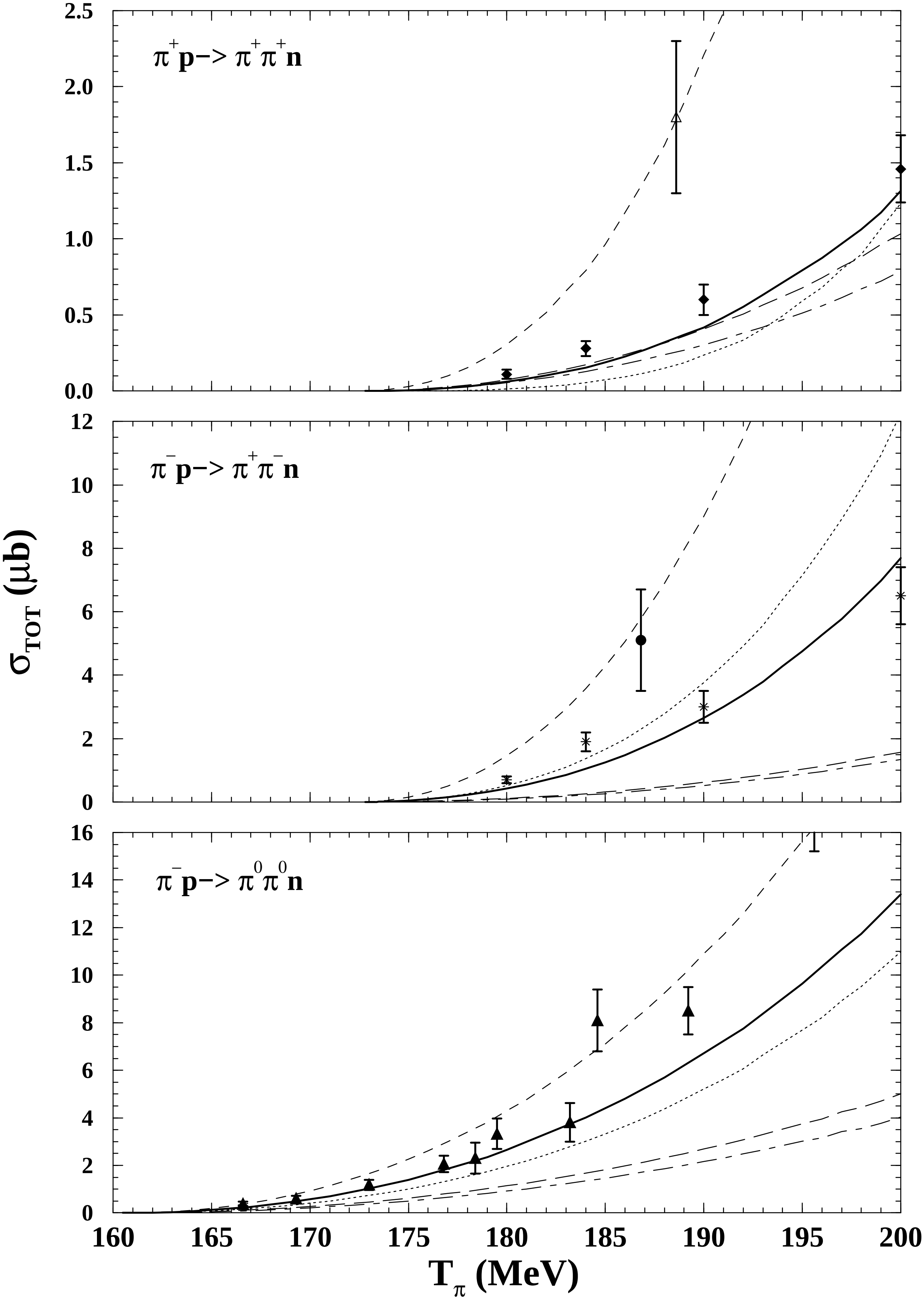

$\pi^+ p \to \pi^+ \pi^+ n$
$\pi^- p \to \pi^+ \pi^- n$
$\pi^- p \to \pi^0 \pi^0 n$
σ_{TOT} (μb)
T_π (MeV)

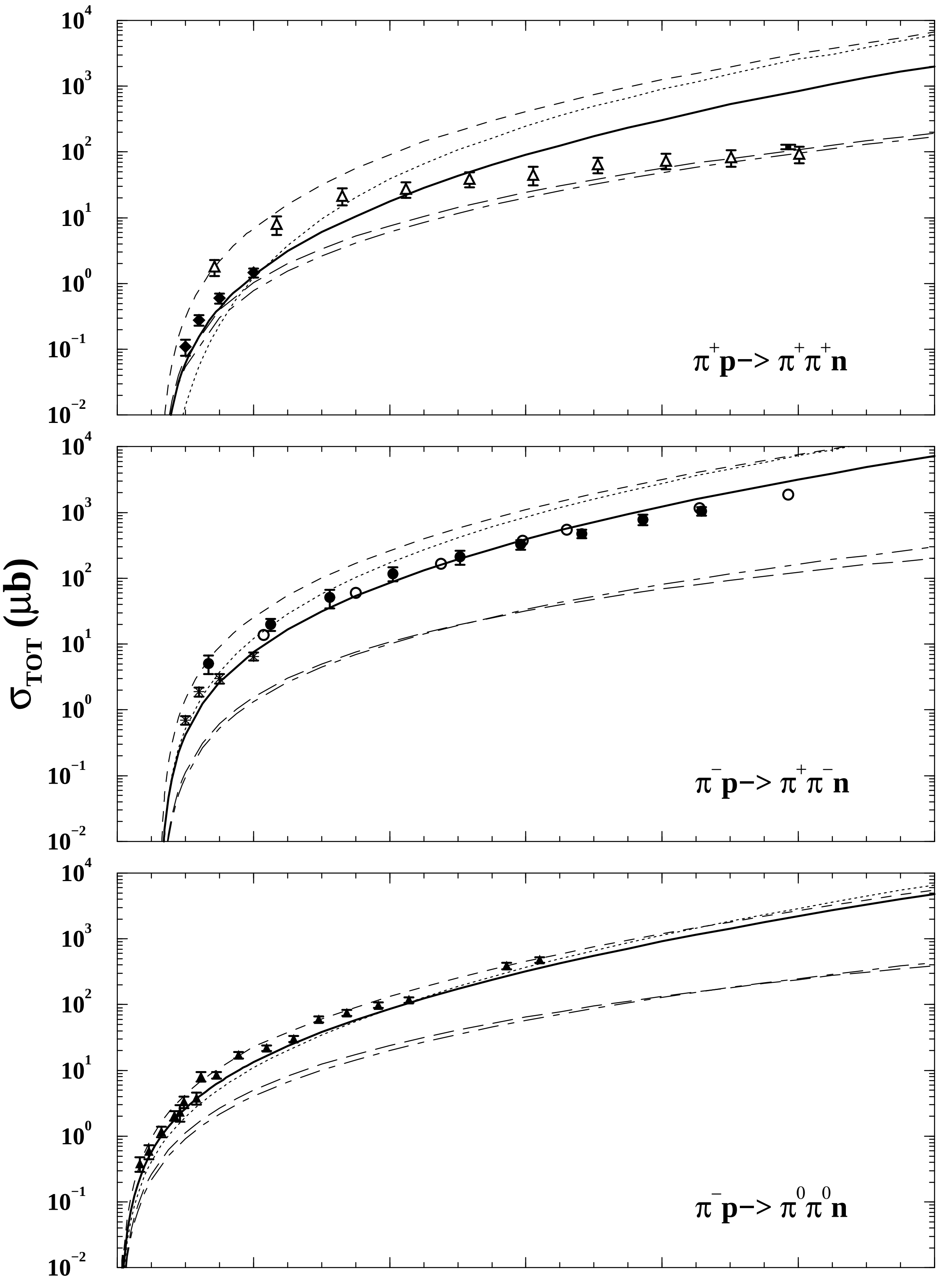

10^4
10^3
10^2
10^1
10^0
10^{-1}
10^{-2}
$\pi^+ p \to \pi^+ \pi^+ n$
$\pi^- p \to \pi^+ \pi^- n$
$\pi^- p \to \pi^0 \pi^0 n$
σ_{TOT} (μb)
160
200
240
280
320
360
400
T_π (MeV)